EAI Endorsed Transactions
on Energy Web
Research Article EAI.EU

Mass Block Stacking Strategy for Efficiency Enhancement of Gravity Energy Storage Systems

Yan Li[1]*, Qingshan Wang[1], Qun Zhang[1], Yifei Fan[1], Darui He[1], Decheng Wang[1], Qiong Wang[1]

[1] State Grid Jiangsu Electric Power Co., Ltd. Economic and Technical Research Institute, Nanjing 210008, China

Abstract

INTRODUCTION: Gravity energy storage systems (GESS) have gained increasing attention because they are less constrained by geography and natural resources, offer flexible capacity expansion, and suit large-scale, long-life, and high-safety applications. However, the growing penetration of intermittent renewable energy increases dispatch frequency and start–stop cycles, making the energy consumption of the stacking (mass-block handling) process a critical factor affecting overall efficiency and cost.
OBJECTIVES: This paper aims to reduce the energy consumption of mass-block stacking operations in GESS, thereby improving system efficiency and supporting the integration of high shares of renewable energy in smart grids.
METHODS: A stacking-zone layout for GESS is designed first. Under given charging/discharging conditions, a nearest-neighbor algorithm is developed to minimize the transporter's energy consumption. For additional (dynamic) charging/discharging conditions, a greedy algorithm with penalty terms is proposed to obtain a low-energy stacking strategy. Case studies are conducted for stacking 100–200 mass blocks (MBs) under given conditions and adding 10–50 MBs under additional conditions of 120 and 150 MBs.
RESULTS: In the simulation cases, compared with the traditional method, the proposed strategy achieves an average energy-saving rate of 25.78% under the given discharge condition. Under additional discharge conditions, the average energy-saving rates are 20.85% (based on 120 MBs) and 16.8% (based on 150 MBs).
CONCLUSION: The proposed stacking-zone design and energy-optimized scheduling strategies effectively reduce stacking energy consumption and enhance the operational efficiency of GESS in grids with intermittent and fluctuating renewable generation, offering a useful reference for future gravity energy storage stacking-system development.

Keywords: Gravity energy storage, Mass block stacking, Path planning, Optimization Strategy

Received on 13 February 2026 accepted on 16 April 2026, published on 23 April 2026

doi: 10.4108/ew.11929

*Corresponding author. Email: liyan239588@126.com

1. Introduction

As the penetration rate of renewable energy in power systems rises, the demand for large-scale energy storage technologies in power grids has become more urgent. Gravity storage is an emerging mechanical energy storage technology. It has gained widespread attention in recent years due to its environmental friendliness, long lifespan, and low cost. Based on differences in the motion trajectory of the mass block (MB), existing gravity energy storage systems (GESS) can be categorized into two types: vertical and inclined[1,2]. Despite different system configurations, the core operating principle is consistent. Electrical power raises the MB from a low potential energy position to a high one to store energy. During discharge, the MB descends and releases potential energy to generate electricity. GESS depend on seamless coordination between multiple components. The stacking process is critical for maintaining normal system operation.

The efficiency and economic viability of GESS are significantly influenced by the MB stacking strategy. In smart grid operating scenarios, load fluctuations and the uncertainty of renewable generation often subject energy storage systems to dynamically changing operating conditions. Energy storage systems therefore need to perform start–stop operations and charge–discharge switching more frequently and to provide multiple services such as peak shaving and frequency regulation, which makes auxiliary losses within the system more likely to be amplified. This often results in added energy losses and response delays. Therefore, developing optimized MB stacking methods that adapt to dynamic grid requirements has significant theoretical value and engineering significance for improving system efficiency.

Current mainstream GESS show significant technical diversity in MB stacking. Energy Vault's tower-based vertical gravity storage system uses a six-degree-of-freedom crane for three-dimensional stacking operations[3,4]. This approach offers high spatial utilization but faces engineering challenges. These include strict positioning accuracy requirements and structural stress concentration in the MBs. To address these, the company's next-generation EVx system uses a rail-based transport vehicle solution[5]. Rigid guide rails confine stacking accuracy to ±5 mm and reduce dynamic loads on MBs by 62%. Elevator-based GESS use SLAM-based automated guided vehicles (AGVs)[6]. These achieve 0.1° attitude control accuracy and 15 ms real-time obstacle avoidance response, though system complexity increases. ARES's rail locomotive system[7,8] attains 15 kWh/m³ volumetric energy density through modular design. Its innovative chain-track structure boosts stacking efficiency to 120 MBs per hour. Suspended cable car systems use gravel media to achieve continuous flow similar to pumped storage[9,10], but their low energy density limits large-scale use. Single-MB shaft solutions, like those in the UK's Gravitricity[11,12], avoid stacking challenges. However, their 250-300 ton composite MBs put high demands on shaft structures and braking systems.

Current research on stacking methods for gravity energy storage is limited. For GESS, which use numerous large-MBs, planning and designing optimal transport routes is critical to ensure operational efficiency. Reference[13] categorizes MBs into four weight tiers and designs their storage area to maximize space. Building on this, it adds constraints on MB transport time and quantity. The study employs the Dijkstra algorithm to plan transport routes for the shortest path. Automated Guided Vehicles (AGVs) are used for collaborative transport. This AGV approach requires pre-drilled holes in the MBs, which significantly increases costs because of the large number of MBs in GESS. In contrast, Reference[14] uses a lifting transfer carrier and dedicated stacking track for MBs to avoid the AGV-related issues. It employs dynamic programming algorithms to find the shortest path for a given discharge scenario. However, when facing additional scenarios, the approach adds a “bypass lane” on the side of the stacking area to resolve MB blockage caused by the initial scenario. This results in additional losses during the additional scenario phase.

To address these issues, this paper focuses on analyzing the design of gravity energy storage stacking zones and corresponding stacking methods. Specifically examining the transportation method using dedicated stacking tracks for lifting transfer transporters and MBs, it investigates the impact of track friction coefficient, track length, and vehicle motor efficiency on the energy consumption of the MB transporter. Based on varying grid demands, a stacking method is proposed that minimizes the operational energy consumption of the MB transporter. Furthermore, a solution achieving minimal energy consumption is presented even under grid demand for additional stacking operations. Case studies are conducted using examples of stacking 100 to 200 MBs under a given condition, with additional stacking of 50 MBs required at 120 and 150 MBs. From a grid-application perspective, the proposed stacking-area design and optimization strategy reduces the energy consumption of the stacking process, thereby enhancing the engineering applicability of gravity energy storage for smart-grid operating scenarios such as peak shaving, frequency regulation, and renewable output smoothing.

2. Basic Principles of Gravity Energy Storage

The following section introduces the principles using a vertical GESS as an example. Among current vertical gravity storage systems, the “matrix” structure proposed by Energy Vault is relatively typical, as shown in Fig. 1[15]. This structure is currently being implemented in a demonstration project by Tianying Company in Rudong, Jiangsu Province. Although both types of gravity storage systems fall under the “vertical” category, their operating principles exhibit slight differences. Their respective working principles are described below.

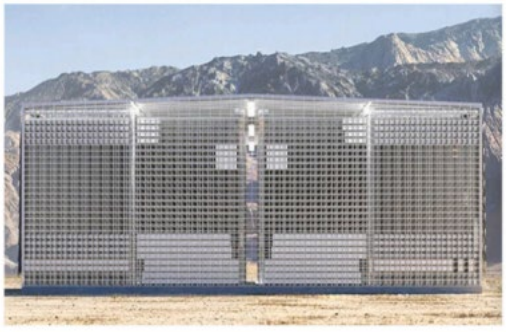

(a) Overall Structure of the Matrix System

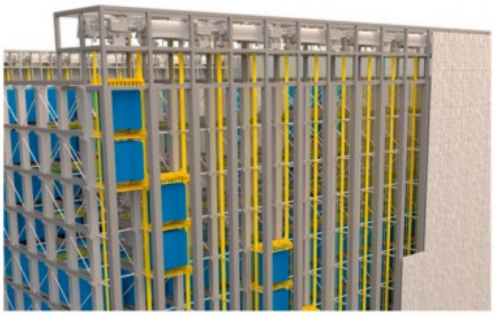

(b) Operational Process of the Matrix System

Figure 1. Matrix-type GESS [15]

The "matrix" structure is based on a steel-framed concrete structure for storing heavy loads in combination with an elevator.

The safety of this structure and the utilization of heavy objects is high. Fig.1. shows the discharge process of the energy storage system from left to right, where heavy objects in the high potential energy position are dragged into the elevator by the traction device, and the elevator descends, dragging the rotor of the motor located at the top of the steel-frame structure to rotate and generate electricity to the power grid, and then the elevator arrives at the low potential energy position, and the heavy objects are moved to the steel-frame structure by the traction device, and then go to the designated stack location. After the elevator reaches the low potential energy level, the weights are moved by the traction device into the steel frame structure and go to the designated stack location. The weights in this structure[16] have a fixed number of layers in the high potential energy position and the low potential energy position to ensure that all the weights store the same amount of power. The charging condition is opposite to the discharging condition and is not described here.

In the development process of energy storage technology, the business model is the key to realizing its maximum utilization value. In different application scenarios, the function of energy storage in the power system is very different: on the power supply side, the primary function of energy storage is peak regulation and frequency modulation; on the grid side, the natural part of energy storage is auxiliary services; on the user side, the primary function of energy storage is system peak shaving. The different process determines remarkable differences in the business models of energy storage in different application scenarios. [17,18]

3. GRAVITY ENERGY STORAGE SYSTEM YARDING AREA DESIGN

3.1. Mass Block Transporter

The MB transporter design incorporates a lifting and transfer mechanism, offering the following advantages:

1) High precision: The lifting and transfer mechanism enables high-precision control, facilitating accurate positioning of MBs during stacking;

2) High flexibility: It can move freely along the stacking zone tracks and return to the transporter docking area via the same route after releasing the MBs;

3) Easy maintenance: Requires lower maintenance frequency and reduced costs;

4) High Speed: Operating faster than overhead cranes, it more readily meets rapid stacking demands for MBs.

Figure 2 illustrates the operational mode of the MB transporter. When transporting MBs along the dual tracks, the lifting and transfer device activates to lift the MB to the designated stacking position. Upon reaching the target location, the device lowers the MB onto the support track.

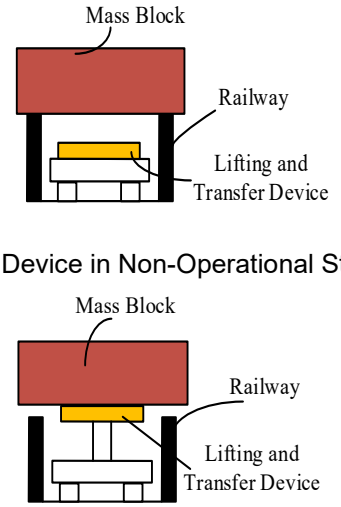

Figure 2. MB Transporter Work Mode Diagram

3.2. Mass Block Stacking Area

For the design of the MB stacking area, the stacking starting point should be positioned at the center of the upper side of the stacking area (as indicated by the green dot in Figure 3.). Construct a track that spans the entire stacking area at its center. No MBs shall be stacked on the cross track. Separate MB stacking support tracks shall be constructed in each column of the remaining white areas. In the case study, a 21 × 21 grid is adopted mainly based on a comprehensive trade-off between demonstrative validation and computational complexity. On the one hand, this grid size provides a sufficient number of stackable positions while still capturing the operational characteristics of stacking strategies in a medium-scale scenario, and is therefore reasonably representative. In the case study, this paper adopts an "empty warehouse" initial state assumption, meaning that all stackable positions are vacant before the task begins and no blocks are pre-occupied. This assumption is primarily introduced to enable a fair comparison of the relative performance of different stacking strategies under a unified initial condition, avoiding the interference of historical stacking configurations on the results. In this way, the effects of the layout design and the algorithmic mechanism itself can be analyzed more clearly.

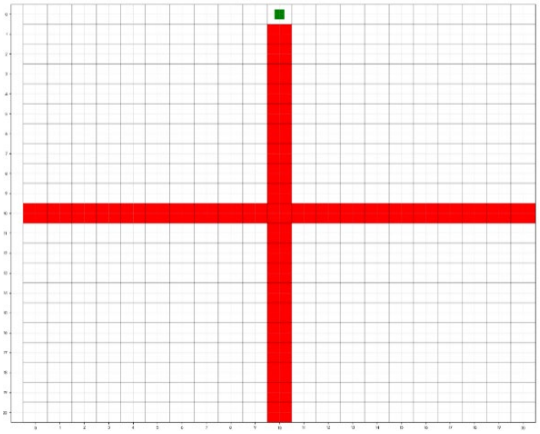

Figure 3. MB Stacking Area Design Diagram

After stacking MBs under specified operating conditions, the MBs accumulate in front of the stacking zone, obstructing subsequent MBs from being placed. Therefore, a red channel is constructed to fulfill the stacking tasks for MBs under additional operating conditions.

The stacking area adopts a single-layer stacking assumption, meaning that each available grid position can accommodate only one mass block (MB), and no vertical stacking is considered. This assumption is intended to avoid introducing complex structural safety issues such as maximum stacking height, load-bearing capacity limits, stability verification, and interlayer interaction constraints. As a result, the focus of the study is placed on planar layout design and transportation path optimization.

The specific parameters of the stacking area are described as follows:

The system considered in this study is a vertical gravity energy storage system with a rated capacity of 1 MW. It is assumed that two mass blocks can operate simultaneously online, with a lifting/lowering speed of 2 m/s.

$$m = \frac{P}{gv} \tag{1}$$

where, m denotes the mass of the block operating simultaneously, P represents the power generation output, and v denotes the operating velocity of the mass block.

Based on the calculation, the mass of each mass block is 25.5 tons. Steel mass blocks are used in this study, and the calculated side length of each block is 1.5 m. Therefore, the side length a of each square grid in the stacking area is 1.5 m. The length of the central rail is the same as the side length of the mass block, which is also 1.5 m.

$$A = n^2 \cdot a^2 \tag{2}$$

where, n represents the total number of stackable blocks in the stacking area, and a denotes the side length of a mass block. The total area of the stacking zone is calculated to be A=992.25m^2.

4. Mass block stacking strategy

4.1. Stack loss analysis

In GESS, the working mechanism of the mass-bearing vehicle is driven by its internal electric motor, which essentially performs work by overcoming friction forces[19,20]. The magnitude of this work is determined by the mass carried by the vehicle and the friction coefficient. Assuming the friction coefficient in both the stacking area and the stacking zone is identical and uniformly denoted as μ, the friction losses during the stacking process can be divided into two components: stacking loss ($Loss_1$) and return loss ($Loss_2$), with their respective expressions as follows.

$$Loss_1 = \frac{\mu(m_0 + M)g}{\eta_L} L_1 \tag{3}$$

$$Loss_2 = \frac{\mu m_0 g}{\eta_{NL}} L_2 \tag{4}$$

where m_0 represents the mass of the transport vehicle, M is the mass of MB, g denotes the gravitational acceleration, L_1 indicates the distance traveled by the transport vehicle during stacking, and L_2 represents the distance covered during return. η_L and η_{NL} denote the efficiency of the onboard motor under loaded and unloaded conditions. The rolling friction coefficient μ between the transporter and the rail in this paper is set to 0.02–0.03, and the transporter mass m_0 is 4 tons. The transporter mass is designed based on the mass of the mass block. Assuming that the motor efficiency does not fluctuate significantly during operation, and noting that μ, g, m_0, M, η_L, and η_{NL} are all greater than zero.

$$\frac{\partial Loss_1}{\partial L_1} = \frac{\mu(m_0 + M)g}{\eta_L} > 0 \tag{5}$$

$$\frac{\partial Loss_2}{\partial L_2} = \frac{\mu m_0 g}{\eta_{NL}} > 0 \tag{6}$$

Therefore, $Loss_1$ and $Loss_2$ are linearly and positively correlated with the travel distances L_1 and L_2, respectively. Hence, the longer the travel distance, the greater the energy loss. Consequently, the key objective of the proposed algorithm is to determine the shortest planned route, thereby improving the operational efficiency of the gravity energy storage system.

The loss model developed in this paper is primarily estimated based on the friction loss and drivetrain efficiency during horizontal travel, with a focus on analyzing the impact of travel distance on the total energy consumption. During the modeling process, additional factors are not further considered, including inertial losses during acceleration and deceleration, energy consumption due to turning, energy consumption during lifting and lowering, as well as transient power variations caused by switching between unloaded and loaded states.

4.2. The nearest neighbor algorithm for a given charge and discharge condition

In conventional gravity energy storage stacking strategies, a sequential filling method is typically adopted, following a back-to-front and center-to-sides order. This approach is mainly designed based on standardized management and spatial sequencing principles, without incorporating factors such as transportation path length, passage occupancy conditions, or the requirements of subsequent incremental tasks into the decision-making process.

In practical operation, such a fixed-order strategy may cause the transporter to frequently travel to distant areas, thereby increasing the average travel distance and energy consumption. Moreover, when additional tasks or dynamic adjustment demands arise, the previously formed centralized stacking pattern may lead to congestion in key passages, ultimately reducing the overall operational efficiency of the system.

GESS can reduce energy consumption during transportation by using algorithms to rationally allocate stacking positions for each MB on every pallet track under given operating conditions. This paper employs the nearest neighbor algorithm under specified charging/discharging scenarios. The algorithm works as follows: Construct the stacking area according to the designed dimensions. Apply constraints[21,22] to the stacking area: cross tracks are prohibited for stacking, and horizontal movement is only permitted on horizontal tracks and the stacking zone at the top of the ramp.

It should be clarified that the term “nearest” in this paper refers to the position closest to the fixed starting point of the system (i.e., the initial position of the lifting transporter).

Under the nearest neighbor algorithm, in each decision step, the moving distance from this fixed starting point to all candidate stacking positions is calculated, and the position with the minimum distance is selected for stacking.

Throughout the entire stacking process, the reference point for distance calculation remains the same fixed starting point, rather than the position of the previously placed mass block. Therefore, “nearest” is defined based on the relative distance to the system’s starting point.

After site initialization, consider the objective function and constraints. Constraints are divided into quantity constraints and area restriction constraints. Quantity constraints ensure the number of placed MBs meets Phase 1 task requirements, while area restriction constraints exclude all positions within restricted zones, ensuring heavy objects are only stacked within permitted available areas. Constraints are as follows:

$$\sum_{p\in P} x_p = K \tag{7}$$

$$x_p = 0, \quad \forall p \in A \tag{8}$$

where K represents the number of weights to be placed in the first stage, P denotes the set of all available positions, p is the coordinate of a single position, and x_p is a binary decision variable valued at 1 when position p is selected and 0 otherwise. A is the set of restricted areas, including passages and other unavailable regions. The objective function for minimizing the energy consumption of the carrier vehicle is as follows:

$$\min_{p\in P} D_1(s,p)\cdot x_p \tag{9}$$

where $D_1(s, p)$ represents the obstacle-free travel distance from starting point s to position p Perform path calculation and priority sorting.

For each available position, execute deterministic path generation and compute the Manhattan distance for each point.

$$d = \left|X - X_p\right| + \left|Y - Y_p\right| \tag{10}$$

where X represents the horizontal coordinate of the starting point of the placement zone, X_p denotes the vertical coordinate of the target position, Y indicates the vertical coordinate of the placement endpoint, and Y_p signifies the vertical coordinate of the target position.

During path planning, due to system constraints limiting horizontal movement to specific channel rows, a rational selection mechanism must be designed to determine the optimal horizontal movement path. The optimal horizontal row $h^*(p)$ is defined as:

$$h^*(p) = \arg\min_{h\in H} |Y_p - h| \tag{11}$$

where h denotes the row number of the channel permitted for horizontal movement, H represents the set of rows in the system permitted for horizontal movement, and Y_p is the vertical coordinate of the target position.

Path Generation Algorithm: Three-Stage Movement Strategy Ensures optimal path generation from start to target position within system constraints. Specific steps are as follows: Vertical Movement Stage:

$$\text{sign}(x) = \begin{cases} 1, & \text{if } x > 0 \\ 0, & \text{if } x = 0 \\ -1, & \text{if } x < 0 \end{cases} \tag{12}$$

$$\Delta_y = \text{sign}(h^*(p) - Y) \tag{13}$$

$$V_1 = \{(X, Y + i\Delta_y) \mid i = 0,1,\ldots, |h^*(p) - Y|\} \tag{14}$$

where Δ_y represents the vertical movement direction, V_1 denotes the set of initial vertical movement path points, and $h^*(p)$-Y indicates the longitudinal movement range.

Horizontal Movement Phase:

$$\Delta_x = \text{sign}(X_p - X_c) \tag{15}$$

$$H = \{X_c + j\Delta_x, h^*(p) \mid j = 0,1,\ldots, |X_p - X_c|\} \tag{16}$$

where Δ_x represents the horizontal movement direction, H denotes the set of path points for horizontal movement. X_c is the horizontal coordinate at the end of vertical movement, and X_p-X_c represents the horizontal movement range.

Final vertical movement segment:

$$\Delta_y' = \text{sign}(Y_p - h^*(p)) \tag{17}$$

$$V_2 = \{X_p, h^*(p) + k\Delta_y' \mid k = 0,1,\ldots, |Y_p - h^*(p)|\} \tag{18}$$

where Δ_y represents the final vertical displacement direction, and Y_p - $h^*(p)$ denotes the final longitudinal displacement range.

Vertical Movement Stage is shown in Figure 4.

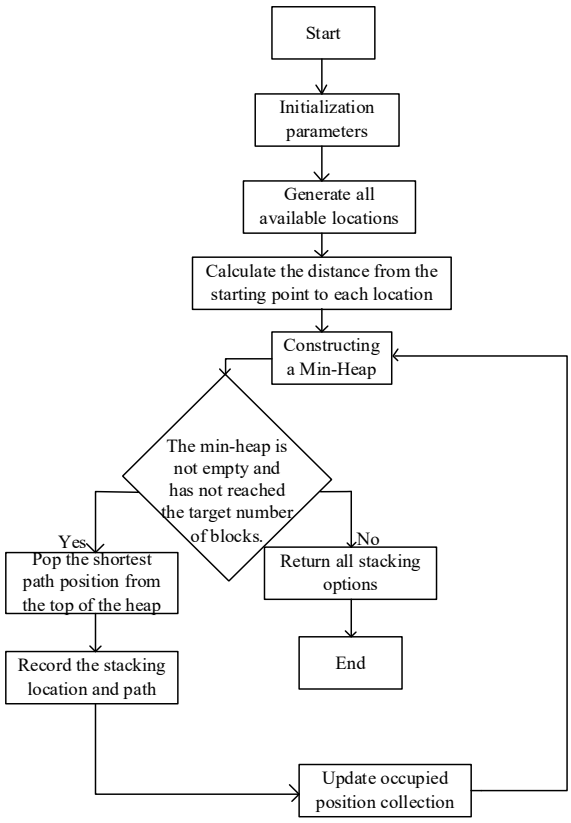

Figure 4. Flow chart of the nearest neighbor algorithm under given conditions

4.3. Greed algorithm term for additional charge-discharge cycles (with penalty)

When a GESS completes a charging/discharging task, if additional tasks are received, some palletizing tracks may already contain stacked MBs. In such cases, these tracks can no longer transport MBs directly. The cross-passageway can deliver MBs to the palletizing zone below using shorter routes. The palletizing method employs a greedy algorithm with penalty terms. The greedy algorithm operates as follows:

First, define the objective function and constraints, where constraints include quantity constraints and location feasibility constraints.

$$\sum_{p\in P_c} y_p = M \tag{19}$$

$$y_p = 0, \quad \forall p \in A \cup P_1 \tag{20}$$

where Pc denotes the candidate position for the mass block, M represents the number of targets, A includes the channel area and other unavailable regions, and P_1 indicates the position where the weight was placed in the first stage. y_p equals 1 if position p is selected for placing the mass block in the second stage, and 0 otherwise.

The objective is to minimize the score, which comprises a path distance term and an obstacle penalty term. The function is defined as follows:

$$\min \sum_{p\in P_c} \text{Score}(p)\cdot y_p \tag{21}$$

$$\text{Score}(p) = D_2(s,p,O) + \omega \cdot \text{ObstacleCount}(p,O) \tag{22}$$

$$\text{ObstacleCount}(p,O) = \sum_{r\in \text{R}(s,p,O)} \text{I}_{\{r\in O \wedge r\neq s \wedge r\neq p\}} \tag{23}$$

where $D_2(s, p, o)$ represents the actual number of steps taken from the starting point to the target position, where s denotes the starting point coordinates, p denotes the target position coordinates, O represents the set of obstacles, ω is the obstacle scoring parameter, ObstacleCount is the number of obstacles encountered along the path (excluding the starting and ending points), and r denotes the coordinates of a single path point along the route.

The second stage employs a greedy selection strategy with penalty terms, treating the MBs placed in the first stage as obstacles and calculating the remaining available positions. Subsequently, the Manhattan distance of the actual path is computed for each candidate. Path determination first checks if a direct path is feasible; if not, a detour path is selected. For placement in the second stage, a dynamic update mechanism is employed: each newly placed block dynamically affects subsequent obstacle detection along paths. A "lazy update" strategy is adopted, avoiding immediate recalculation of all paths. The total score for candidate positions is the sum of the base distance score and the obstacle penalty score. The base distance score is the Manhattan distance of the actual path. The obstacle penalty score adds two points for each obstacle crossed. After calculating the scores for each placement position, the position with the lowest total score is prioritized. In case of a tie, the position with fewer obstacles is chosen. Finally, a suitable placement area is selected. The priority of each position is determined by the scoring function. Below is the iterative function: First, arrange the set of positions P in order of priority based on the optimal comprehensive scores:

$$P = \{p_{(1)}, p_{(2)}, \ldots, p_{(M)}\} \tag{24}$$

$$P_{(i)} = \arg\min \mathbf{Score}(p)_{p\in S_{i-1}} \tag{25}$$

$$S_i = \begin{cases} P_c, & i = 0 \\ S_{i-1} / \{P_{(i)}\}, & i \geq 1 \end{cases} \tag{26}$$

where $P(i)$ denotes the position selected in the iteration, S_{i-1} represents the set of remaining candidate positions before the i-th selection, Score(p) is the comprehensive scoring function for position p, and S_i denotes the set of remaining candidates after the i-th selection.

The process of the greedy algorithm under specified conditions is illustrated in Figure 5.

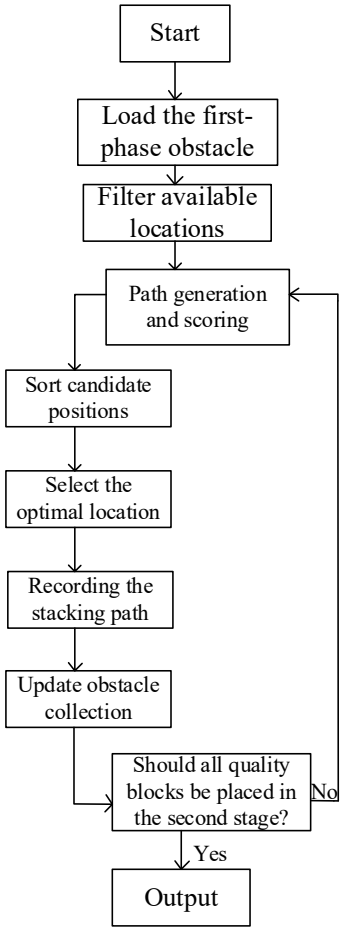

Figure 5. Flow chart of the greedy algorithm under specified conditions

5. Case Analysis

5.1 Given charge-discharge conditions

In this case, the stacking area has a length and width of 21 grids. Each grid cell represents one unit length. The cross track divides the stacking area into four equal parts below the starting point. The stacking quantity is set to 100, 110, 120, 130, 140, 150, 160, 170, 180, 190, and 200 MBs respectively. After simulation, the total distance of the transporter vehicle after comparing the optimized strategy with the traditional strategy is shown in Table 1:

Table 1. Performance Comparison of Optimization Strategy and Traditional Strategy.

Number of stacked MBs	Total distance of the vehicle (one unit length)	
	optimization strategy	traditional strategy
100	1540	2340
110	1764	2710
120	2004	2880
130	2256	3250
140	2516	3420
150	2796	3810
160	3084	4000
170	3384	4390
180	3700	4580
190	4024	4990
200	4364	5200

This study takes the stacking of 120 MB as an example for analysis, as shown in Figures 6 and 7.

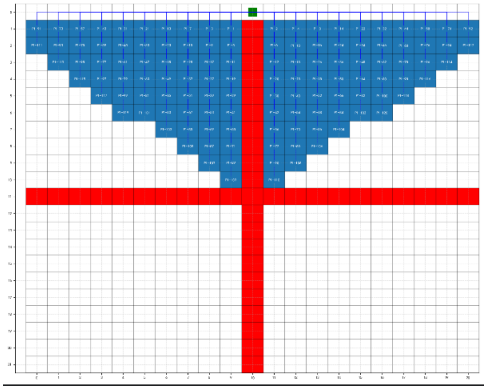

Figure 6. Stacking 120 MBs under the optimization strategy

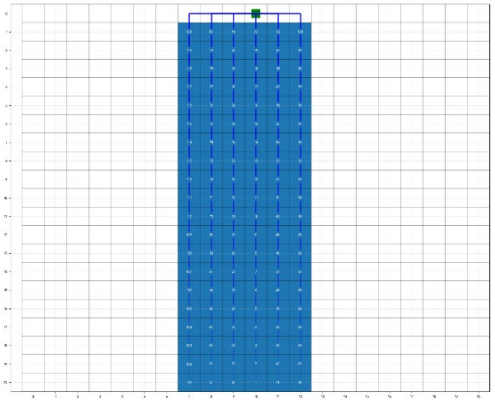

Figure 7. Stacking 120 MBs under the traditional strategy

The traditional stacking method places MBs starting from the starting point, stacking them sequentially from the rear to the front in columns closest to the starting point. The optimized method, by stacking according to nearest-neighbor placement, avoids crossing cross passages during the first stacking phase. As shown in Table 1, the optimized strategy

achieves significantly shorter travel distances for the load-bearing vehicle compared to the traditional strategy. This improvement stems from the optimized method's sequential stacking approach, which allows the vehicle to traverse longer distances when the storage path remains partially unoccupied. Figure 8 presents a comparative line graph illustrating the movement distance differences between the two strategies. Under these operating conditions, the average energy savings rate is 25.78%.

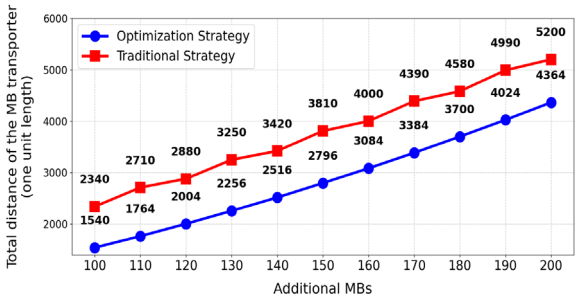

Figure 8. Comparison of the moving distance of the MB transporter between the optimization and traditional strategy

5.2 During additional charging and discharging

In this computational case study, we conducted comparative analyses of total movement distances between the optimization strategy and traditional strategy by incrementally adding 10, 20, 30, 40, and 50 additional MBs to the baseline configurations of 120 MBs and 150 MBs under specified working conditions. Figure 9 and Figure 10 demonstrate the simulation results of the strategy when 30 extra MBs are added to the initial 120 MBs setup.

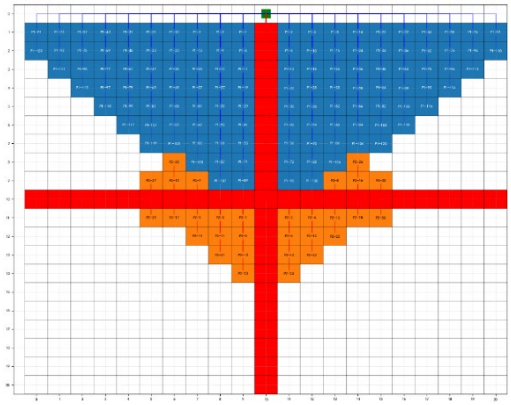

Figure 9. Simulation of 120 stacked MBs and 30 additional MBs under optimization strategy

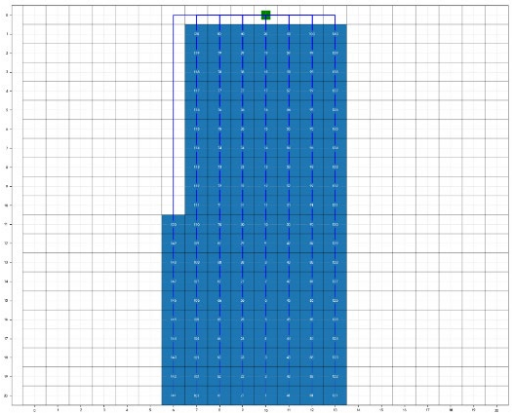

Figure 10. Simulation of 120 stacked MBs and 30 additional MBs under traditional strategy

The distance between the optimized strategy and the traditional strategy for stacking additional MBs based on the stacked 120 and 150 MBs is shown in Table 2 and Table 3, respectively.

Table 2. The distance between the optimized strategy and the traditional strategy for stacking additional MBs based on the stacked 120 MBs

Additional MBs	Total distance of the MB transporter (one unit length)	
	optimization strategy	traditional strategy
10	2308	3250
20	2640	3420
30	2992	3810
40	3356	4000
50	3736	4390

Table 3. The distance between the optimized strategy and the traditional strategy for stacking additional MBs based on the stacked 150 MBs

Additional MBs	Total distance of the MB transporter (one unit length)	
	optimization strategy	traditional strategy
10	3120	4000
20	3476	4390
30	3852	4580

40	4244	4990
50	4648	5200

It is obvious from the comparison of the data in Table 2 and Table 3 that the moving distance of the vehicle carried by the optimization strategy is less than that of the traditional strategy. The comparison chart of the total moving distance of the MB transporter carried by the additional strategy and the traditional strategy is shown in Figure 11 and Figure 12.

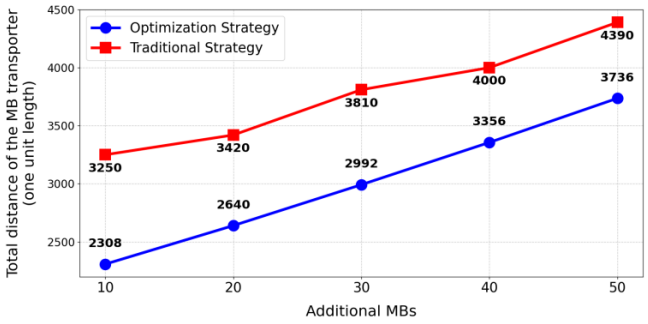

Figure 11. Total stacking distance comparison of MB transporter between the optimization strategy and the traditional strategy based on the stacked 120 MBs

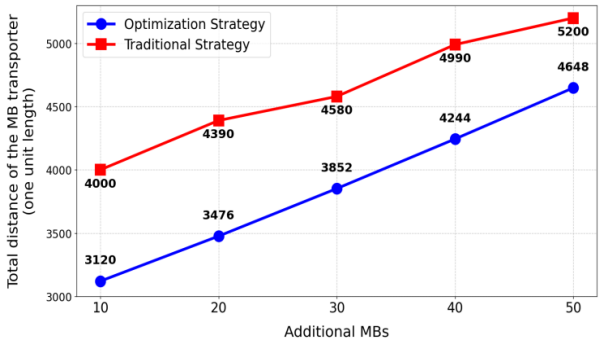

Figure 12. Total stacking distance comparison of MB transporter between the optimization strategy and the traditional strategy based on the stacked 150 MBs

After determining the total travel distances under the two algorithms, the next key performance indicator to consider is the energy utilization efficiency during system operation, namely, the energy-saving rate.

$$\eta = \frac{E_t - E_o}{E_t} \times 100\% \tag{27}$$

where E_t represents the total travel distance under the traditional strategy, E_o represents the total travel distance under the optimized strategy, and η denotes the energy-saving rate.

In the traditional stacking method, MBs in the second stage are still placed sequentially from the rear to the front of the columns closest to the starting point. In contrast, the optimized method uses cross-channels to stack MBs at the bottom of the upper two stacking zones and the top of the lower two stacking zones. As shown in Figure 11 and Figure 12, for a given 120-MBs stack configuration, the distance savings achieved by the optimization strategy compared to traditional methods gradually decrease from 29% to 14.9% as the number of added MBs increases sequentially. However, the total movement distance remains lower under the traditional strategy. Under these operating conditions, the average energy savings rate is 20.85%. For a 150-MBs stack configuration with progressively added MBs, the distance savings diminish from 22% to 10.6% as the MB count increases. Nevertheless, the overall distance savings still outperform the traditional strategy, maintaining an advantage over conventional methods. Under these operating conditions, the average energy savings rate is 16.8%.

6. Conclusion

This paper addresses the high energy consumption issue in GESS's MB stacking by designing a specialized stacking area. Two strategies are proposed for the designed stacking zone, aiming to minimize energy consumption of the MB transport vehicle under both given charging/discharging scenarios and additional charging/discharging tasks. The conclusions are as follows:

(i) A cross-shaped stacking area with through-track design is developed. The strategy constraints during stacking processes are analyzed under given and additional charging/discharging tasks. Two optimization strategies are proposed to achieve minimum energy consumption for both scenarios.

(ii) Case studies are conducted with 100-200 MBs under given tasks and 50 additional MBs under 120-150 MB conditions. Results show that compared to traditional methods, the proposed approach achieves an average energy saving rate of 25.78% for given discharge tasks. Under 120 MB conditions with additional discharge tasks, the method achieves 20.85% average energy saving, while under 150 MB conditions with additional discharge tasks, the average energy saving rate reaches 16.8%.

Finally, despite achieving certain energy-saving effects, this study has the following limitations: the research primarily targets palletizing zones with specific layouts, and its adaptability to other structural configurations requires further validation; optimization analysis was conducted solely for single-mass-block carrier vehicle transportation, while actual systems typically involve multiple carrier vehicles operating collaboratively, neglecting multi-vehicle scheduling and path coordination issues. Based on current findings, future research directions include: exploring universal optimization strategies for diverse stacking zone layouts, conducting collaborative scheduling and path planning studies for multi-carrier systems, and enhancing the practical applicability of strategies. This study provides a theoretical foundation and methodological support for optimizing the energy consumption of the stacking process in

gravity energy storage systems. By reducing auxiliary losses during stacking, it also helps alleviate response lag under dynamic operating conditions and improve dispatch adaptability, thereby having positive significance for promoting the practical application of gravity energy storage technology in power grids.

Acknowledgements

This work is supported by the State Grid Jiangsu Power Co, LTD. Science and Technology Project under Grant No. J202

References

[1] Wang Z, Yu X, Dong L., et al. Key Parameters Design of Chain-Rail Based Slope Gravity Energy Storage System for Optimal Efficiency. IEEE Transactions on Industry Applications, 2026, 62(1): 1349-1358.

[2] Morstyn T, Chilcott M, McCulloch M D. Gravity energy storage with suspended weights for abandoned mine shafts. Applied energy, 2019, 239: 201-206.

[3] Andrade J E, Rosakis A J, Conte J P, et al. Seismic Performance Assessment of Multiblock Tower Structures As Gravity Energy Storage Systems. ASME J. Appl. Mech., 2021.

[4] Aneke, Mathew, and Meihong Wang. Energy storage technologies and real life applications–A state of the art review. Applied Energy 2016, 179: 350-377

[5] Kavoosi, A., and M. Tarafdar Hagh. Solid gravity energy storage: Pioneering energy storage solution–A review. Journal of Energy Storage, 2025, 113: 115691.

[6] Hunt, Julian David, et al. Lift Energy Storage Technology: A solution for decentralized urban energy storage. Energy, 2022, 254(PA): 124102.

[7] Cava, Francesca, et al. Advanced rail energy storage: green energy storage for green energy. Storing Energy, 2016, 69-86.

[8] Hunt, Julian David, et al. Electric truck gravity energy storage: An alternative to seasonal energy storage. Energy storage, 2024, 6(1).

[9] Optimistic, T. G. Gravel energy storage system funded by Bill Gates. The Green Optimistic, 2015.

[10] Hunt, Julian David, et al. Mountain Gravity Energy Storage: A new solution for closing the gap between existing short-and long-term storage technologies. Energy, 2020, 190: 116419.

[11] Morstyn, Thomas, Martin Chilcott, and Malcolm D. McCulloch. Gravity energy storage with suspended weights for abandoned mine shafts. Applied energy, 2019, 239: 201-206.

[12] Hunt J D, Jurasz J, Zakeri B, et al. Underground Gravity Energy Storage: A Solution for Long-Term Energy Storage. Energies (Basel). 2023; 16: 825.

[13] Zeng X, Jiang J, Li J, et al. Storage and Transportation Solutions for Heavy Material Blocks in 100 MWh Vertical Shaft Gravity Energy Storage Systems. Energy Storage Science and Technology. 2025; 14:3839-3847 .

[14] Wang Z, Wu G, Zhang Y, et al. Dynamic Programming-Based Mass Block Stacking Method of Gravity Energy Storage System for Minimum Energy Consumption. IEEE Transactions on Industry Applications. 2025; 61: 9628 - 9639.

[15] Tong W., Lu Z., Chen W, et al. Solid gravity energy storage: A review. Journal of Energy Storage . 2022; 53.

[16] Haider S, Shahmoradi-Moghadam H, Schonberger J O, et al. Algorithm and Optimization Model for Energy Storage Using Vertically Stacked Blocks. IEEE Access. 2020; 8: 217688–217700.

[17] Chen J, Zhang X, Peng X, et al. Efficient Routing for Multi-AGV Based on Optimized Ant-Agent. Computers & Industrial Engineering. 2022; 167.

[18] Fan H, Peng W, Ma M, et al. Storage Space Allocation and Twin Automated Stacking Cranes Scheduling in Automated Container Terminals. IEEE Transactions on Intelligent Transportation Systems. 2021; 23:14336–14348.

[19] Karuppiah N, Mounica P, Bhanutej J.N, et al. Revolutionizing Renewable Energy Integration: The Innovative Gravity Energy Storage Solution E3S Web of Conferences. 2024; 547: 3028.

[20] Cao Y, Yang A, Liu Y, et al. AGV Dispatching and Bidirectional Conflict-Free Routing Problem in Automated Container Terminal. Computers & Industrial Engineering. 2023; 184: 109611.

[21] Botha C.D., and M.J. Kamper. Capability Study of Dry Gravity Energy Storage. Journal of Energy Storage. 2019; 23:159–174.

[22] Wang W, Peng Y, Xu X, et al. Smart Container Port Development: Recent Technologies and Research Advances. Intelligent Transportation Infrastructure. 2024; 3.